Supplementary Material for:

Publisher: Elsevier

Journal: Journal of Hydrology

DOI: 10.1016/j.jhydrol.2022.128100

The impact of evaporation fractionation on the inverse estimation of soil hydraulic and isotope transport parameters

Tiantian Zhou[1*], Jirka Šimůnek[1*], Isabelle Braud[2], Paolo Nasta[3], Giuseppe Brunetti[4], and Yi Liu[5]

[1] Department of Environmental Sciences, University of California Riverside, CA 92521, United States
[2] INRAE, Riverly, 5 Rue de la Doua, 69625 Villeurbanne, Cedex, France
[3] Department of Agricultural Sciences, AFBE Division, University of Naples Federico II, Portici (Naples), Italy
[4] Institute of Hydraulics and Rural Water Management, University of Natural Resources and Life Sciences, 1190, Vienna, Austria
[5] China Institute of Geo-Environment Monitoring, China Geological Survey, Beijing, 100081, China

Tables

Table S1. Summary of the observed data in the Stumpp et al. (2012) dataset.

Indicators	Depth (cm)	Frequency	Period
Weather	-	Daily	Whole period
Isotopic composition of precipitation	-	Event	Whole period
Soil water content	10, 15, 25, 45, 70, 100, and 130	Daily	Starting in 2004
Soil retention curve	20, 40, and 100	Once, to obtain $\theta(h)$	At the end of the observation period in 2007
Bottom water flux	-	Weekly	Whole period
Isotopic composition of drainage	-	Weekly	Whole period

Note that soil retention curves were measured using laboratory drainage experiments on the 100-cm^3 soil samples collected at depths of 20, 40, and 100 cm, while the time series of soil water contents were measured in-situ at depths of 10, 15, 25, 45, 70, 100, and 130 cm.

Table S2. Initial and reduced ranges of parameters used in the Stumpp et al. (2012) dataset.

Parameter	Initial range	Reduced range
θ_{s1} [-]	0.3-0.6	0.3-0.5
α_1 [1/cm]	0.001-0.3	0.001-0.2
n_1 [-]	1.1-2.0	1.1-1.4
K_{s1} [cm/d]	10-220	10-220
λ [cm]	1.0-20	5.0-20
θ_{s2} [-]	0.3-0.6	0.4-0.6
α_2 [1/cm]	0.001-0.3	0.1-0.3
n_2 [-]	1.1-2.0	1.1-1.4
K_{s2} [cm/d]	10-12000	10-9000
θ_{s3} [-]	0.3-0.6	0.3-0.6
α_3 [1/cm]	0.001-0.3	0.001-0.3
n_3 [-]	1.1-2.0	1.1-2.0
K_{s3} [cm/d]	10-220	10-220

Table S3. Sobol' sensitivity analysis indices for the Stumpp et al. (2012) dataset. S_{1_bf}, S_{1_wc}, S_{1_wi}, S_{1_rc}, S_{1_avg}, S_{T_bf}, S_{T_wc}, S_{T_wi}, S_{T_rc}, and S_{T_avg} represent the first-order (subscript 1) and total (subscript *T*) variances for the time series of the bottom flux (subscript *bf*), the soil water content (subscript *wc*) at different depths, and the bottom water isotopic composition (subscript *wi*), as well as the water retention curves (subscript *rc*), and the overall averages (subscript *avg*), respectively.

Parameter	S_1_*bf*	S_1_*bf* (BCI)	S_T_*bf*	S_T_ *bf* (BCI)
α_1	0.499	0.028	0.611**	0.031
n_1	0.228	0.022	0.286*	0.013
θ_{s1}	0.111	0.013	0.135	0.006
α_3	0.017	0.010	0.048+	0.003
K_{s1}	0.001	0.005	0.020	0.002
α_2	0.003	0.005	0.018	0.002
K_{s2}	0.002	0.004	0.014	0.002
K_{s3}	0.002	0.004	0.012	0.001
n_2	0.001	0.003	0.005	0.000
θ_{s2}	0.001	0.002	0.004	0.000
θ_{s3}	0.000	0.002	0.002	0.000
n_3	0.000	0.001	0.001	0.000
λ	0.000	0.000	0.000	0.000
Sum	0.865		1.155	
Parameter	S_1_*wc*	S_1_ *wc* (BCI)	S_T_*wc*	S_T_ *wc* (BCI)
n_2	0.187	0.023	0.350	0.017
n_1	0.059	0.017	0.229	0.013
α_2	0.042	0.018	0.215	0.014
α_3	0.075	0.017	0.185	0.015
n_3	0.019	0.015	0.142	0.011
θ_{s3}	0.035	0.013	0.133	0.008
θ_{s1}	0.009	0.015	0.125	0.007
θ_{s2}	0.017	0.012	0.099	0.006
α_1	0.010	0.012	0.079	0.007
K_{s1}	0.008	0.008	0.045	0.004
K_{s2}	0.011	0.006	0.024	0.004
K_{s3}	0.000	0.005	0.016	0.004
λ	0.000	0.000	0.000	0.000
Sum	0.473		1.643	
Parameter	S_1_*wi*	S_1_ *wi* (BCI)	S_T_*wi*	S_T_ *wi* (BCI)
n_2	0.122	0.016	0.247	0.018
n_3	0.076	0.017	0.185	0.012
α_2	0.058	0.014	0.169	0.013
λ	0.073	0.017	0.168	0.009
θ_{s3}	0.089	0.014	0.165	0.009
α_1	0.059	0.012	0.137	0.011
n_1	0.061	0.014	0.118	0.007
θ_{s2}	0.033	0.008	0.074	0.005

α_3	0.018	0.009	0.071	0.007
θ_{s1}	0.043	0.012	0.066	0.004
K_{s3}	0.011	0.007	0.032	0.003
K_{s2}	0.008	0.005	0.019	0.003
K_{s1}	0.000	0.004	0.015	0.003
Sum	0.651		1.466	
Parameter	S_1_rc	S_1_ rc (BCI)	S_T_ rc	S_T_rc (BCI)
n_2	0.184	0.022	0.352	0.019
n_3	0.073	0.023	0.293	0.016
n_1	0.112	0.020	0.246	0.012
α_3	0.040	0.020	0.229	0.013
α_2	0.036	0.015	0.189	0.011
α_1	0.009	0.015	0.135	0.009
θ_{s3}	0.000	0.010	0.070	0.003
θ_{s1}	0.001	0.011	0.066	0.005
θ_{s2}	0.005	0.010	0.062	0.004
K_{s1}	-0.002	0.004	0.013	0.004
K_{s3}	0.001	0.002	0.004	0.003
K_{s2}	0.001	0.001	0.002	0.002
λ	0.000	0.000	0.000	0.000
Sum	0.461		1.659	
Parameter	S_1_avg	S_1_ avg (BCI)	S_T_ avg	S_T_avg (BCI)
n_2	0.219	0.025	0.386	0.020
n_1	0.124	0.018	0.267	0.013
n_3	0.037	0.016	0.218	0.012
α_2	0.044	0.017	0.203	0.013
α_3	0.022	0.018	0.178	0.010
α_1	0.015	0.012	0.119	0.009
θ_{s1}	-0.002	0.011	0.079	0.006
θ_{s3}	0.002	0.011	0.078	0.004
θ_{s2}	0.010	0.010	0.072	0.005
K_{s1}	0.000	0.005	0.016	0.004
K_{s3}	0.001	0.003	0.006	0.004
K_{s2}	0.003	0.003	0.005	0.003
λ	0.000	0.001	0.001	0.000
Sum	0.475		1.628	

[+]Red fonts indicate the first-order or total indices within 1%~10%

*Purple fonts indicate the first-order or total indices within 10%~50%

[**]Blue fonts indicate the first-order or total indices larger than 50%

Table S4. Initial and reduced ranges of parameters used in the Braud et al. (2009a) dataset.

Parameter	Initial range	Reduced range
θ_s [-]	0.38-0.48	0.38-0.48
α [1/cm]	0.008-0.011	0.008-0.011
n [-]	2.2-2.6	2.2-2.6
K_s [cm/d]	0.1296-0.216	0.1296-0.216
λ [cm]	0.1-1	0.1-1

Table S5. Sobol' sensitivity analysis indices for the Braud et al. (2009a) dataset. S_{1_wc}, S_{1_wi}, S_{1_avg}, S_{T_wc}, S_{T_wi}, and S_{T_avg} represent the first-order (subscript 1) and total (subscript *T*) variances for the final soil water content profile (subscript *wc*), the water isotopic composition profile (subscript *wi*), and the overall averages (subscript *avg*), respectively.

Parameter	S_{1_wc}	S_{1_wc} (BCI)	S_{T_wc}	S_{T_wc} (BCI)
n	0.379	0.038	0.691**	0.075
θ_s	0.309	0.036	0.596	0.045
λ	-0.006	0.019	0.495*	0.813
α	0.003	0.007	0.080+	0.063
K_s	0.008	0.007	0.078	0.064
Sum	0.693		1.940	
Parameter	S_{1_wi}	S_{1_wi} (BCI)	S_{T_wi}	S_{T_wi} (BCI)
n	0.379	0.035	0.691	0.065
θ_s	0.309	0.032	0.596	0.041
λ	-0.006	0.016	0.497	0.742
α	0.003	0.008	0.080	0.052
K_s	0.008	0.008	0.079	0.050
Sum	0.693		1.943	
Parameter	S_{1_avg}	S_{1_avg} (BCI)	S_{T_avg}	S_{T_avg} (BCI)
n	0.629	0.038	0.975	0.039
θ_s	0.019	0.025	0.350	0.017
K_s	0.016	0.008	0.060	0.005
α	0.003	0.006	0.025	0.002
λ	0.003	0.004	0.011	0.002
Sum	0.670		1.421	

+Red fonts indicate the first-order indices within 1%~10%

*Purple fonts indicate the total indices within 10%~50%

**Blue fonts indicate the total indices larger than 50%

Figures

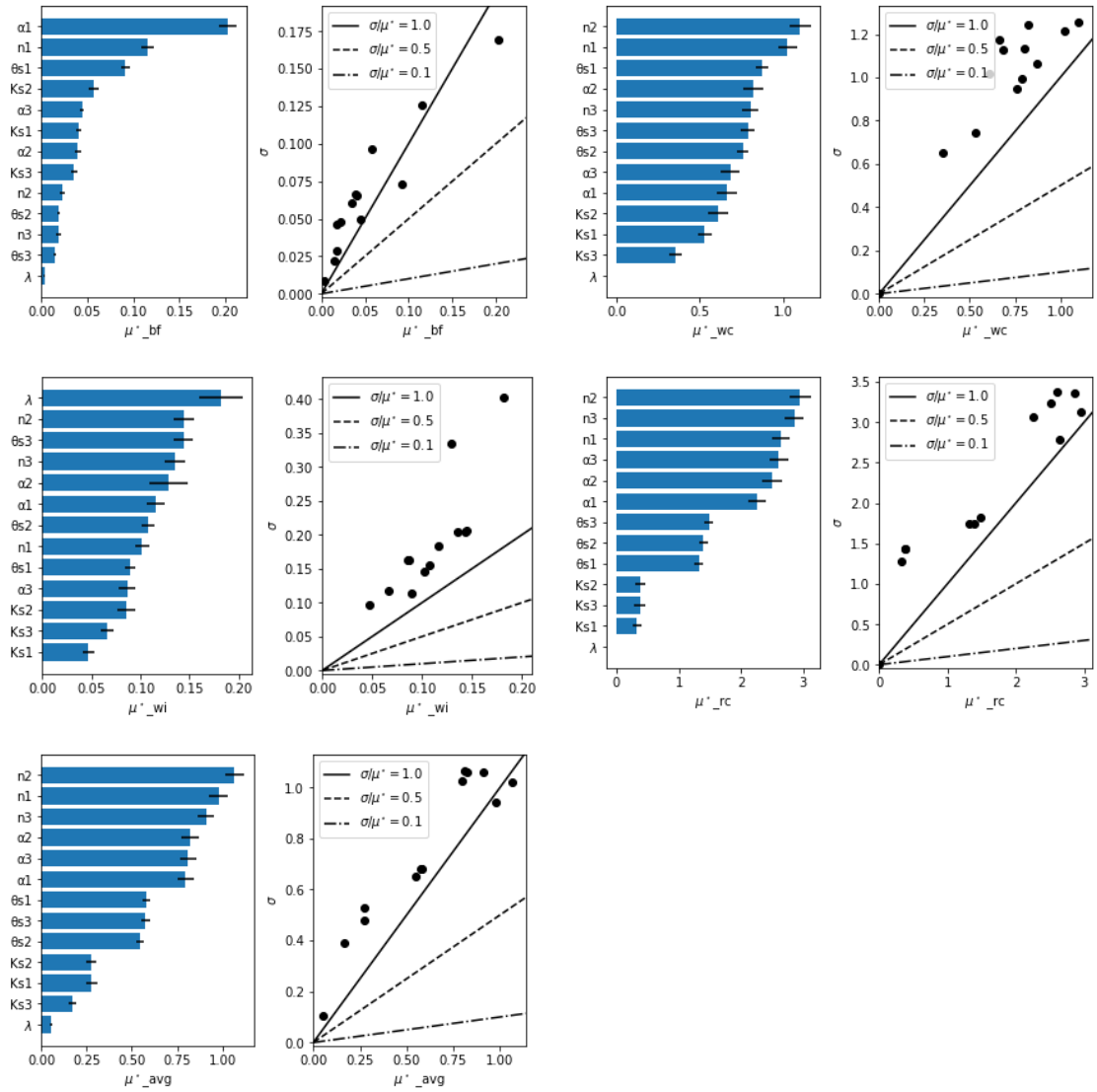

Figure S1. The μ_j^* and $\mu_j^* \sim \sigma_j$ plots for the Morris sensitivity analysis for the bottom water flux (subscript *bf*, top left), soil water content (subscript *wc*, top right), the isotopic composition of the discharge (subscript *wi*, middle left), water retention curve (subscript *rc*, middle right), and the overall averages (subscript *avg*, bottom left) for the Stumpp et al. (2012) dataset.

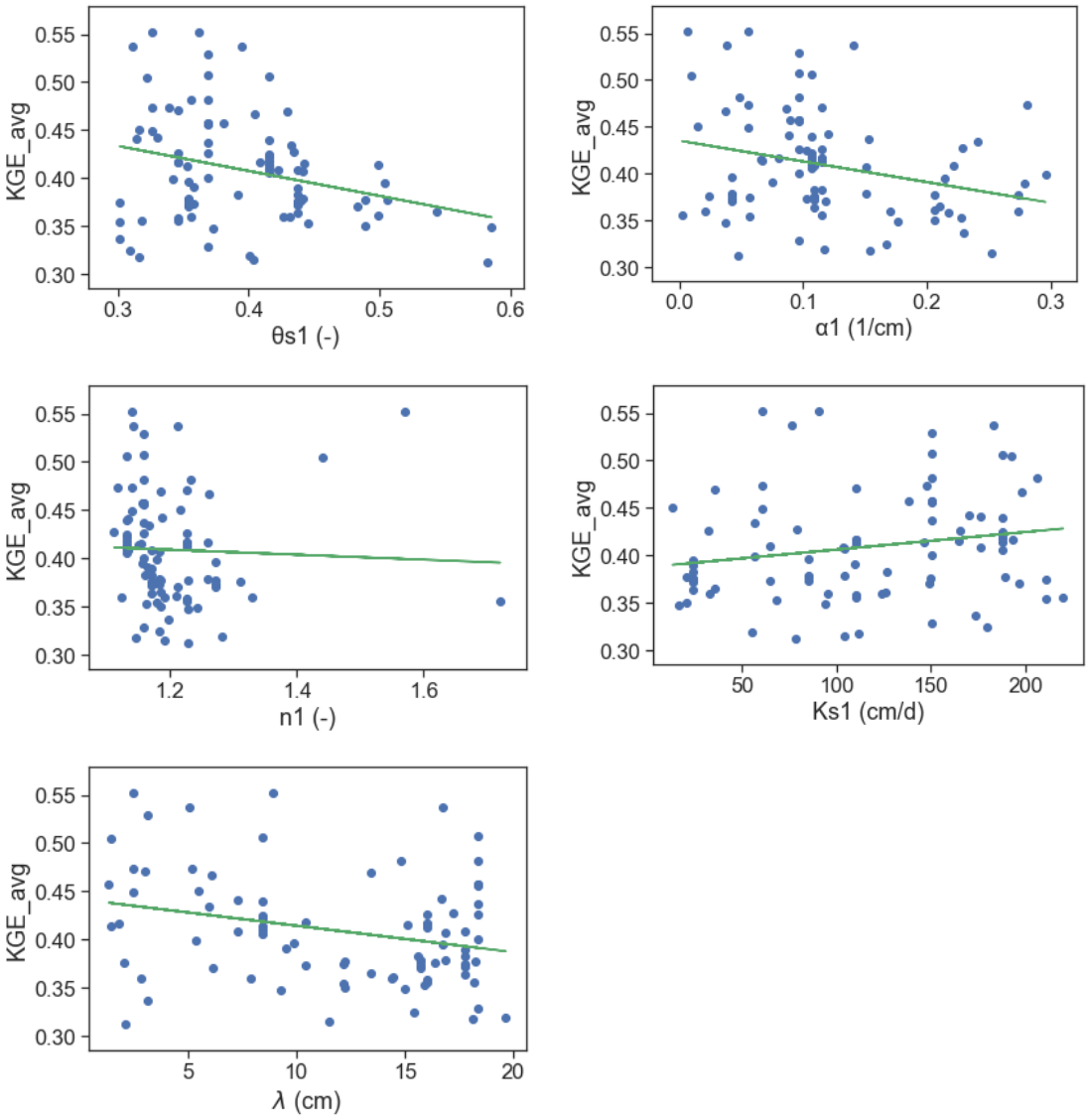

Figure S2. Scatter plots for pair relations θ_{s1}-KGE, α_1-KGE, n_1-KGE, and K_{s1}-KGE for the average performance for the Stumpp et al. (2012) dataset.

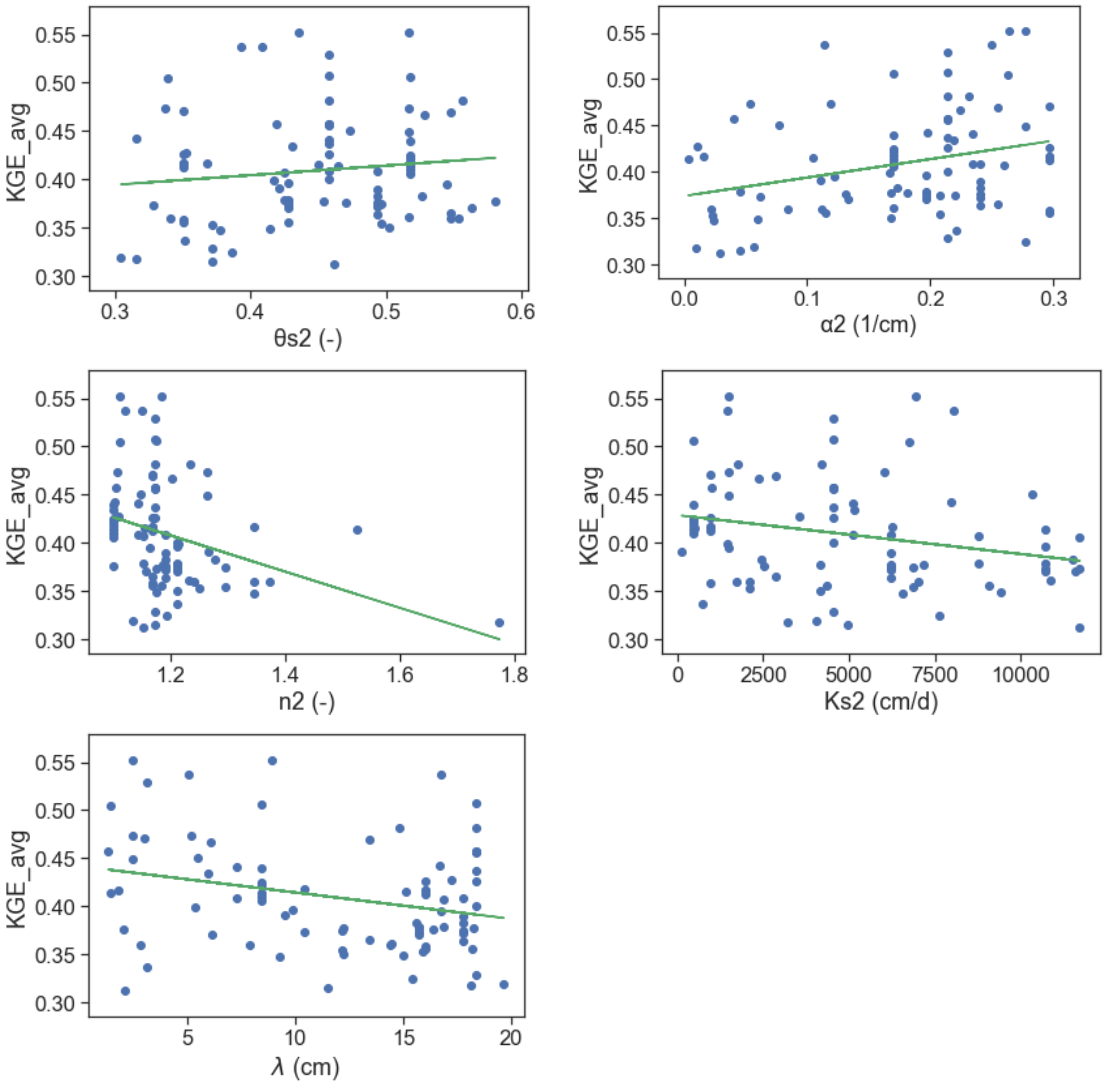

Figure S3. Scatter plots for pair relations θ_{s2}-KGE, α_2-KGE, n_2-KGE, and K_{s2}-KGE for the average performance for the Stumpp et al. (2012) dataset.

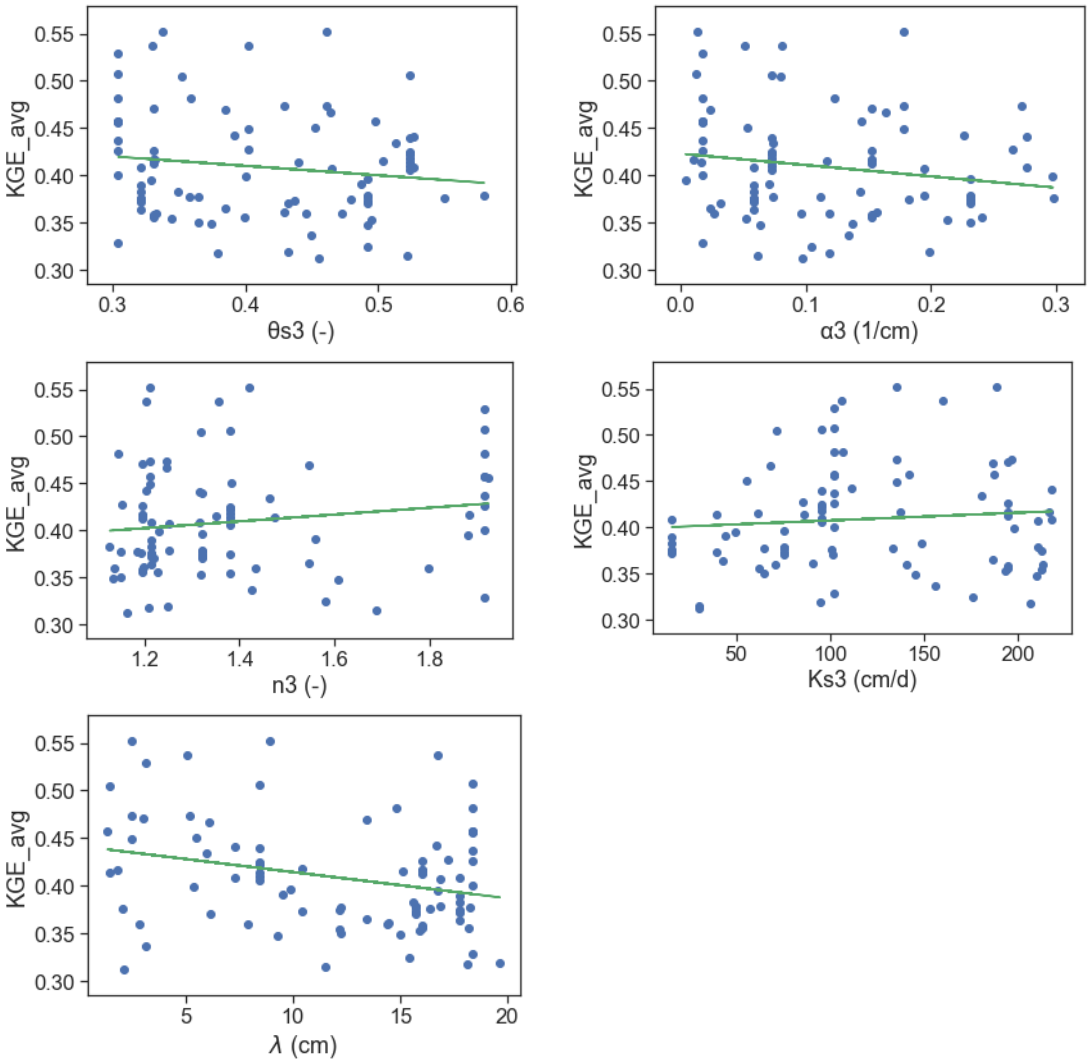

Figure S4. Scatter plots for pair relations θ_{s3}-KGE, α_3-KGE, n_3-KGE, and K_{s3}-KGE for the average performance for the Stumpp et al. (2012) dataset.

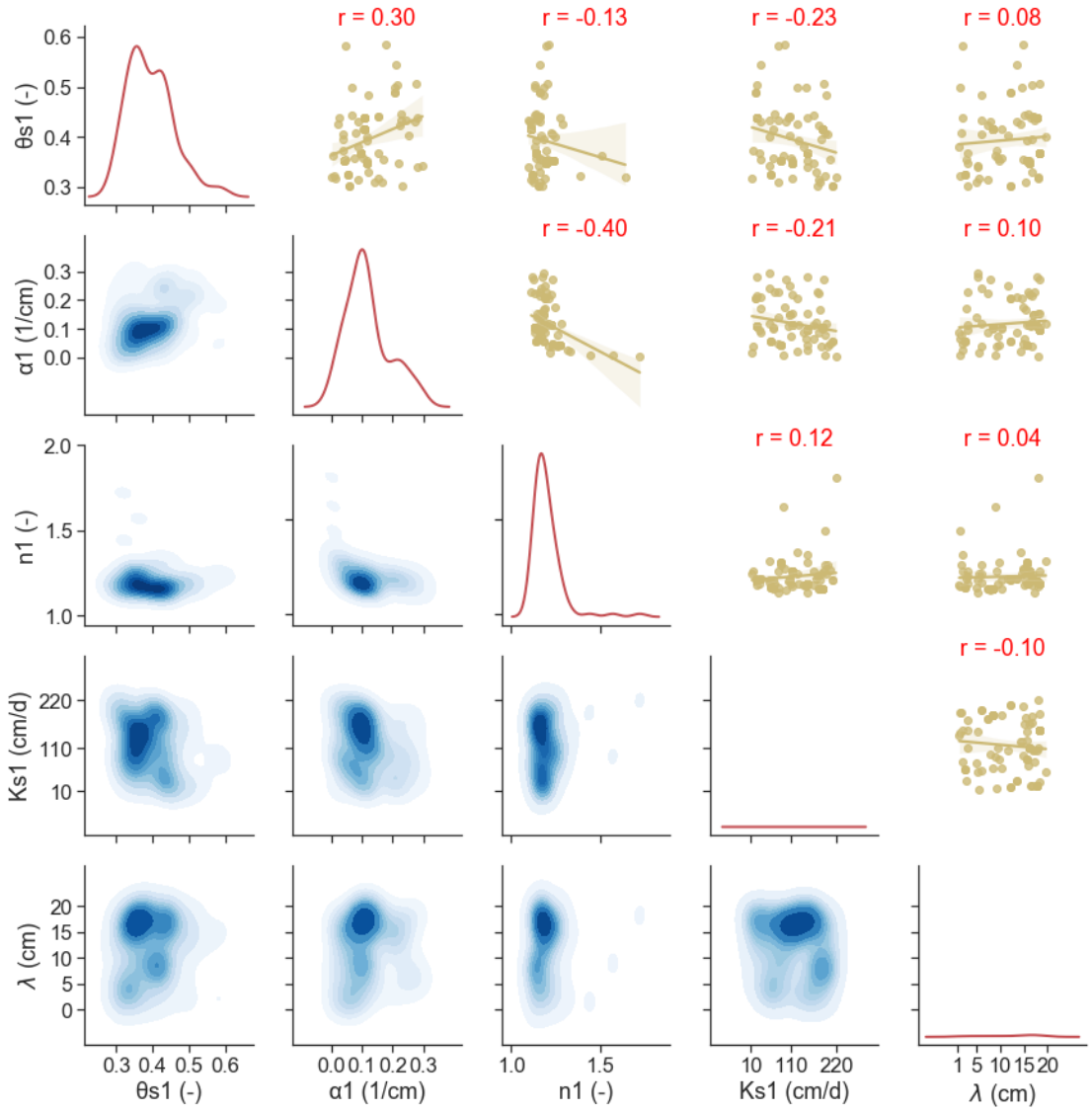

Figure S5. Bivariate KDE plots (below diagonal), univariate KDE plots (diagonal), and correlation plots (above diagonal) for the parameters of the first soil layer (0-30 cm) (for the Stumpp et al. (2012) dataset).

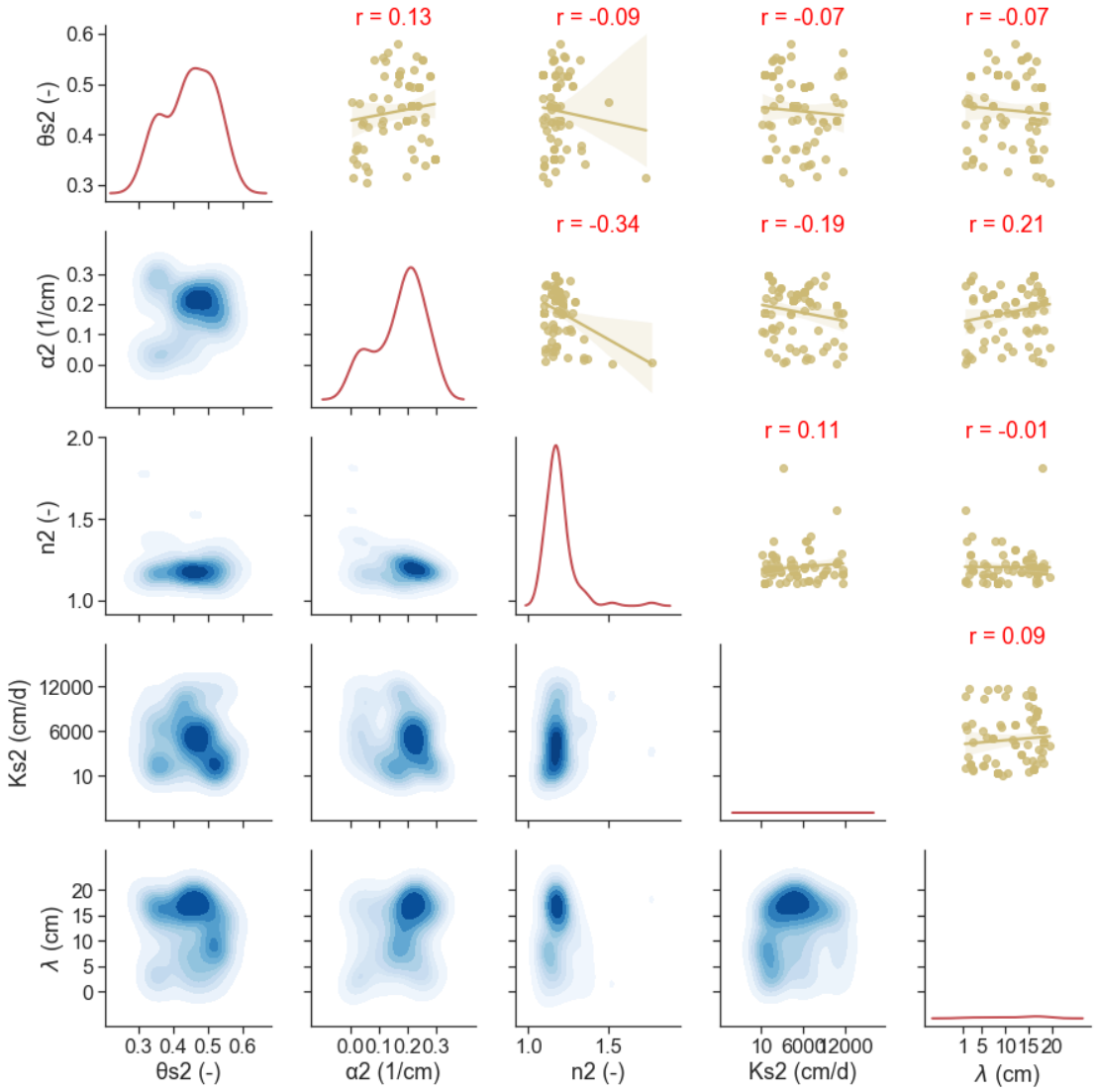

Figure S6. Bivariate KDE plots (below diagonal), univariate KDE plots (diagonal), and correlation plots (above diagonal) for the parameters of the second soil layer (30-90 cm) (for the Stumpp et al. (2012) dataset).

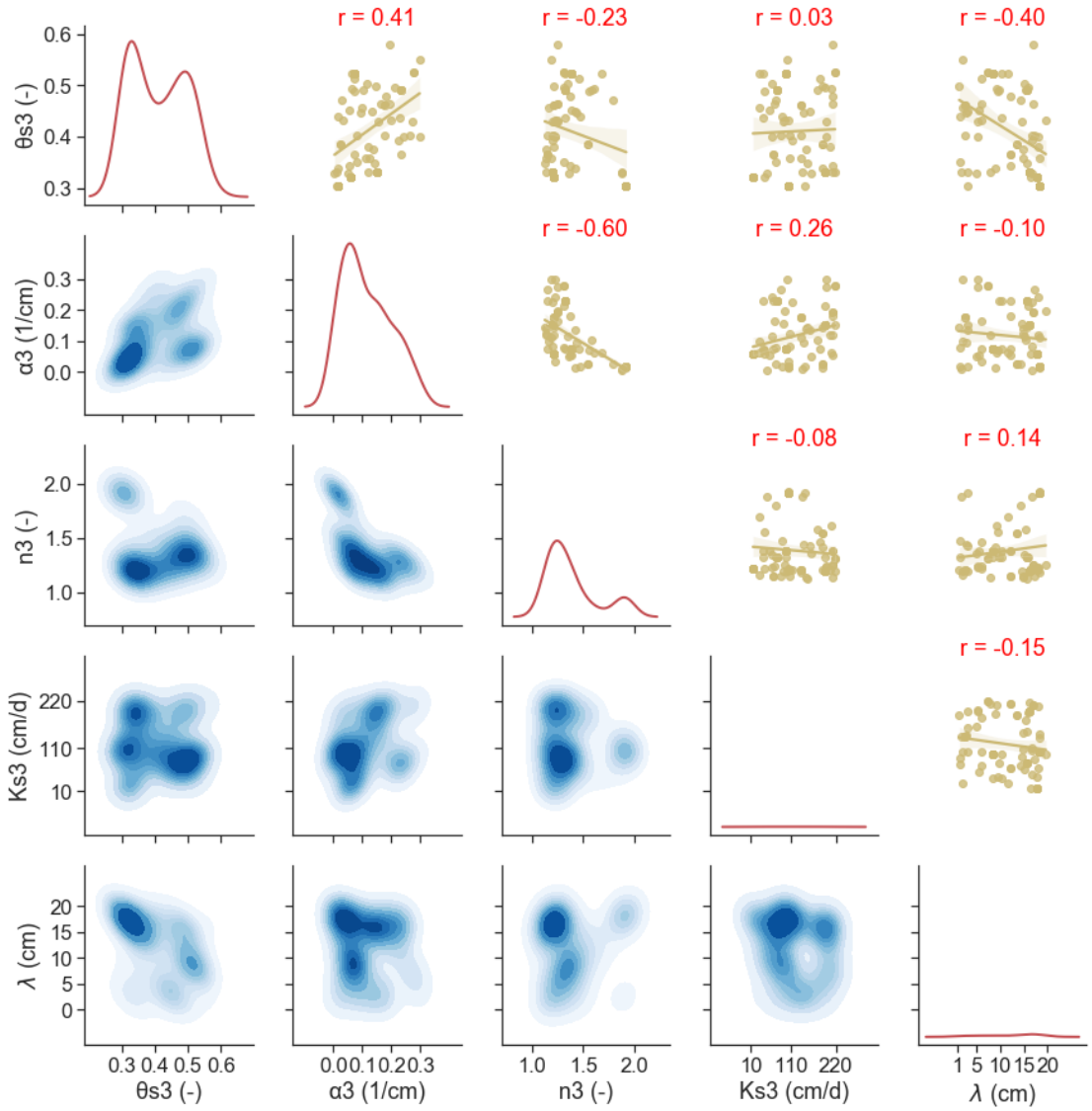

Figure S7. Bivariate KDE plots (below diagonal), univariate KDE plots (diagonal), and correlation plots (above diagonal) for the parameters of the third soil layer (90-150 cm) (for the Stumpp et al. (2012) dataset).

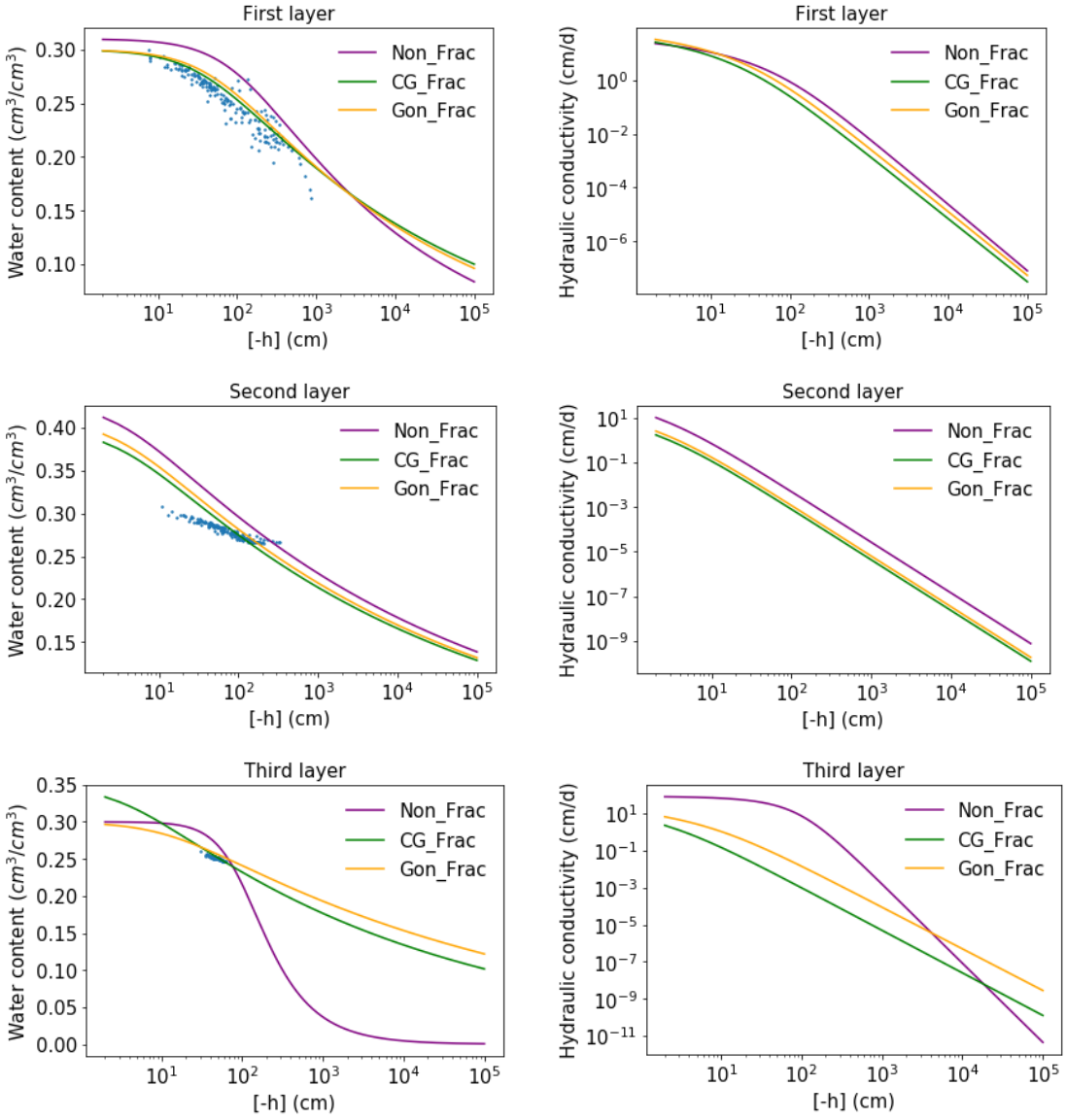

Figure S8. The soil water retention (left) and hydraulic conductivity (right) curves for different layers (first layer - top, second layer - middle, and third layer - bottom) and different fractionation scenarios for the Stumpp et al. (2012) dataset.

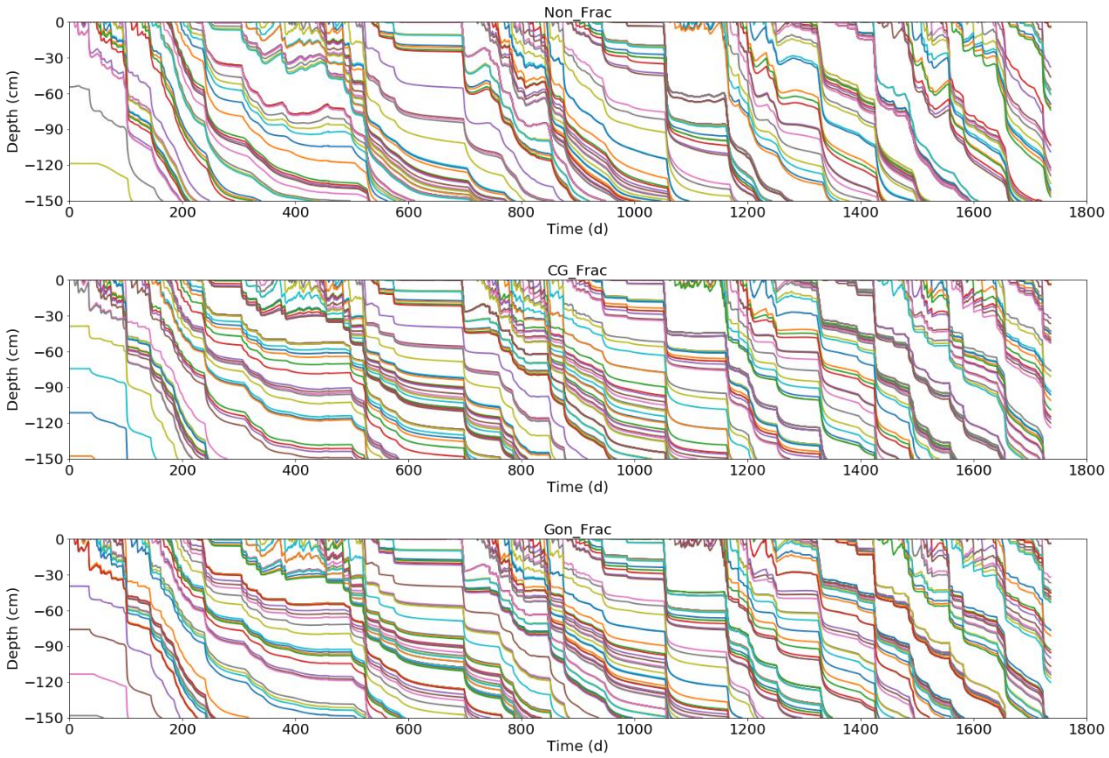

Figure S9. The particle trajectories simulated using the soil hydraulic parameters estimated assuming different fractionation scenarios (Non_Frac – top, CG_Frac – middle, and Gon_Frac – bottom).

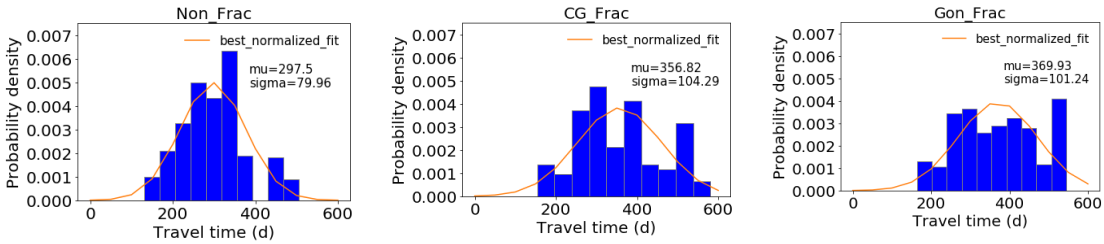

Figure S10. The probability density distribution of water travel times calculated using the soil hydraulic parameters estimated assuming different fractionation scenarios (Non_Frac – left, CG_Frac – middle, and Gon_Frac – right).

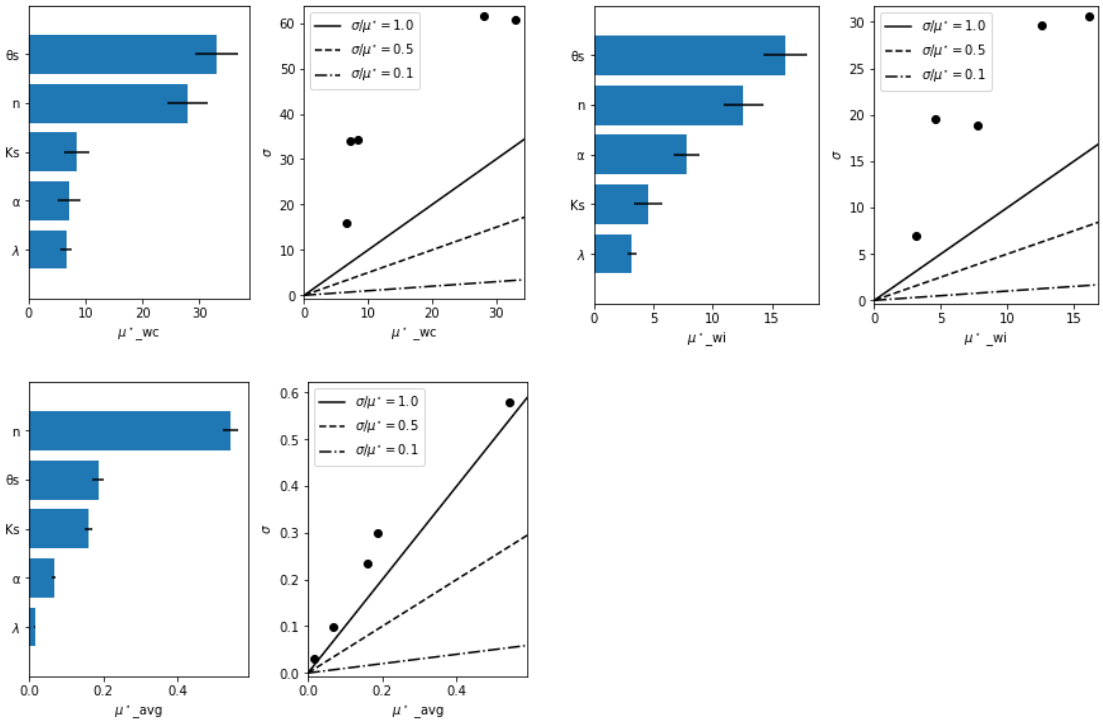

Figure S11. The μ_j^* and $\mu_j^* \sim \sigma_j$ plots for the Morris sensitivity analysis for the soil water content (subscript *wc*, top left), isotopic composition (subscript *wi*, top right), and average (subscript *avg*, bottom) for the Braud et al. (2009a) dataset.

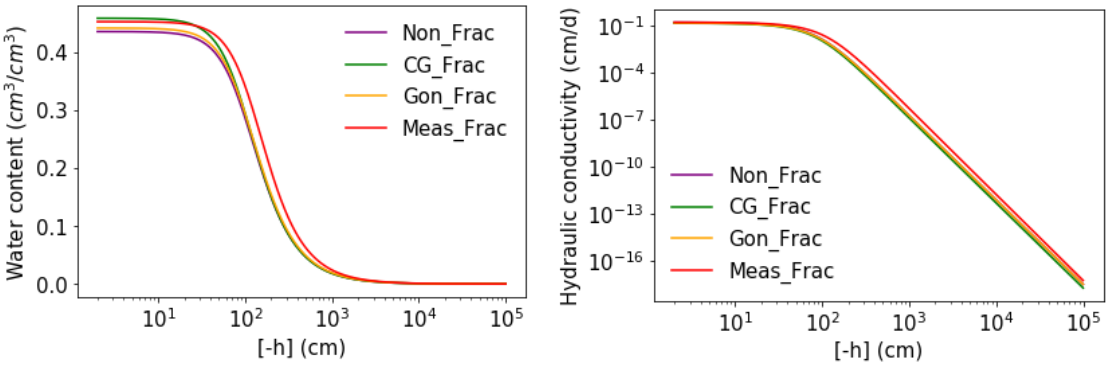

Figure S12. The soil water retention (left) and hydraulic conductivity (right) curves for different fractionation scenarios for the Braud et al. (2009a) dataset.

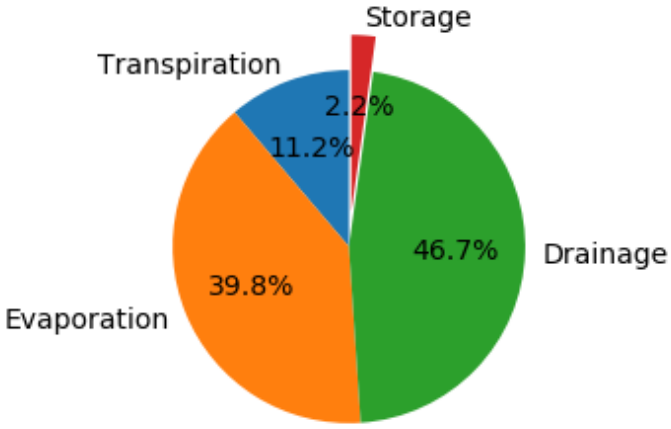

Figure S13. Precipitation contributions to different water balance components in the Non_Frac scenario for the Stumpp et al. (2012) dataset.

Method S1: Evaporation fractionation models

S1.1 Craig-Gordon model

The isotope flux of evaporation E_i (kg/m^2/s) is:

$$E_i = \frac{E}{\alpha_i^k}\frac{M_i}{M_w}\frac{(H_{rs}\cdot\alpha^+\cdot R_L - h_a'\cdot R_a)}{H_{rs}-h_a'} \quad \text{(S1)}$$

The isotope ratio of the evaporation flux R_E (-) is:

$$R_E = E_i/E = [H_{rs}\cdot\alpha^+\cdot R_L - h_a'\cdot R_a]/[(H_{rs}-h_a')\cdot\alpha_i^k]\cdot\frac{M_i}{M_w} \quad \text{(S2)}$$

where E is the evaporation flux, H_{rs} [-] is the relative humidity of the surface soil air phase, h_a' [-] is the normalized air relative humidity, R_L is the isotope ratio of the remaining surface liquid water [-], R_a is the isotope ratio of the atmospheric water vapor [-], and α^+ and α_i^k [-] are the equilibrium and kinetic fractionation factors, respectively.

S1.2 Gonfiantini model

The total fractionation factor (α_i^{total}) can be simplified as (Gonfiantini, 1986):

$$\varepsilon_k = 1000 * \left(\alpha_i^k - 1\right) * (H_{rs} - h_a') \quad \text{(S3)}$$

$$\alpha_i^{total} = 1/\alpha_i^* + \frac{\varepsilon_k}{1000} \quad \text{(S4)}$$

The isotope ratio of the evaporation flux (R_E) is then calculated as:

$$R_E = R_L/\alpha_i^{total} \quad \text{(S5)}$$

More details about different fractionation models can be found in Section 3 of Zhou et al. (2021).

Method S2: Global sensitivity analysis methods

S2.1 Morris method

The Morris method is a screening-based method that performs a one-at-a-time (OAT) analysis. By randomly selecting the initial X on the grid points and constructing a randomized trajectory in this grid structure, r trajectories can be obtained, which scan the entire input parameter space. Along the trajectory i, each parameter X_j is varied along a size Δe_j to explore its influence on the model output Y. This means that each sample differs by only one coordinate (only one parameter is changed) from the previous sample. This relative variation of the model output for parameter X_j is called the elementary effect E_j^i, which can be calculated as:

$$E_j^i = \frac{Y(X + e_j\Delta) - Y(X)}{e_j\Delta} \tag{S5}$$

where Y is the model output corresponding to parameter set X, Δ is a value chosen in the range of $\{1/(k-1), \ldots, 1-1/k-1)\}$, in which k is the number of discretization levels, and e_j is a vector of zeros, but with a unit as its j-th component.

Two indices, μ_j^* and σ_j, are then computed to evaluate the sensitivity order of the input parameters:

$$\mu_j^* = \frac{1}{r}\sum_{i=1}^{r} |E_j^i| \tag{S6}$$

$$\sigma_j = \sqrt{\frac{1}{r}\sum_{i=1}^{r} (E_j^i - \frac{1}{r}\sum_{i=1}^{r} E_j^i)^2} \tag{S7}$$

where the former estimates the direct effect of the parameter X_j on the model output, and the latter represents the indirect effect or interaction effects with other parameters. More details can be found in (Campolongo et al., 2007).

In this study, $r = 1000$ was chosen, which is much higher than the recommended value (more than 20~30) suggested by Herman et al. (2013). The model runs were 14000 (i.e., 1000*(13+1)) and 6000 (i.e., 1000*(5+1)) for the Stumpp et al. (2012) and Braud et al. (2009a) datasets, respectively.

S2.2 Sobol' method

The Sobol' method is a variance-based method that quantifies the contribution of the change of each parameter to the model output variance. The sensitivity indices (SIs) are expressed as:

$$\text{First-order indices: } S_{1,j} = \frac{V_j}{V} \tag{S8}$$

$$\text{Second-order indices: } S_{j,i} = \frac{V_{ji}}{V} \tag{S9}$$

$$\text{Total indices: } S_{Tj} = S_{1,j} + \sum_{i \neq j} S_{j,i} \tag{S10}$$

where V_j is the variance caused by the j-th parameter, and V is the total variance.

First-order indicators $S_{1,j}$ represent the direct contribution of the variance of an individual parameter X_j to the total unconditional variance (namely the direct effect). The second-order indices $S_{j,i}$ explain the contribution of the interaction between parameters X_j and X_i. The total effect of parameter X_j is denoted by the total index S_{Tj} that includes the direct and indirect effects. More details can be found in Sobol' (2001).

The total number of samples q = 5000 as recommended (less than 5000) by Nossent et al. (2011) was chosen in this study. The model runs were 75000 ($5000 * (13 + 2)$) and 35000 (i.e., 5000*(5+2)) for the Stumpp et al. (2012) and Braud et al. (2009a) datasets, respectively. The bootstrap confidence intervals (BCIs) were also estimated to evaluate the accuracy of the sensitivity indices.

Results S1: Global sensitivity analysis and Monte-Carlo filtering for the Stumpp et al. (2012) dataset

S1.1 Global sensitivity analysis

a. Morris method

Table S2 provides the initial ranges of all evaluated parameters. Fig. S1 reports the order of parameters sensitive to bottom water fluxes (KGE_bf), soil water contents (KGE_wc), isotopic compositions of the discharge (KGE_wi), water retention curves (KGE_rc), and the overall averages (KGE_avg), respectively. It can be seen from the μ_j^* values for the bottom flux that α_1 and n_1 show the most significant direct effects on the outputs, followed by θ_{s1} and K_{s_2}. For the soil water contents, n_2 and n_1 show the most significant direct effects on the outputs, followed by θ_{s_1} and α_2. For the isotopic compositions of discharge, λ and n_2 show the most significant direct effects on the outputs, followed by θ_{s_3} and n_3. For the water retention curves, n_2 and n_3 show the most significant direct effects on the outputs, followed by n_1 and α_3. For the average performance, n_2 and n_1 show the most significant direct effects on the outputs, followed by n_3 and α_2.

In general, all parameters with high direct effects (large μ_j^*) often have high indirect effects (large σ_j). The $\mu_j^*{\sim}\sigma_j$ values plotted around and above the 1:1 line suggest that the indirect effects or interactions between parameters are close to or more significant than the direct effects.

Overall, as seen from the μ_j^* and $\mu_j^*{\sim}\sigma_j$ plots of the KGE_avg, soil hydraulic parameters of different layers have comparable impacts on the model outputs. The order of sensitive parameters is: shape parameters *n*, shape parameters α, saturated water contents θ_s, saturated hydraulic conductivities K_s, and dispersivities λ.

b. Sobol' method

Table S3 reports sensitivity indices for the bottom water flux (KGE_bf), the soil water content (KGE_wc), the isotopic composition of the bottom flux (KGE_wi), water retention curve (KGE_rc), and the average (KGE_avg). For KGE_bf, the α_1, n_1, and θ_{s1} parameters show a relatively significant direct effect (50%, 23%, and 11%,

respectively). Other parameters have first-order indices less than 10%, indicating that their direct effect on the variance of KGE_bf is relatively small. The sum of all first-order indices is less than 1, and about 87% of the variance is caused by the direct effects, suggesting that the interactions between parameters are relatively small. About 61% of the variance of KGE_bf is caused by α_1, followed by n_1 (29%) and θ_{s1} (14%), either by the direct effect or interactions with other parameters.

For KGE_wc, the n_2 parameter shows a relatively significant direct effect (19%). Other parameters have first-order indices less than 10%, indicating that their direct effect on the variance of KGE_wc is relatively small. The sum of all first-order indices is less than 1, and about 47% of the variance is caused by the direct effects, suggesting that the interactions between parameters are very important. About 35% of the variance of KGE_wc is caused by n_2, followed by n_1 (23%) and α_2 (22%), either by the direct effect or interactions with other parameters.

For KGE_wi, the n_2 parameter shows a relatively significant direct effect (12%). Other parameters have first-order indices less than 10%, indicating that their direct effect on the variance of KGE_wi is relatively small. The sum of all first-order indices is less than 1, and about 65% of the variance is caused by the direct effects, suggesting that the interactions between parameters are very important. About 25% of the variance of KGE_wi is caused by n_2, followed by n_3 (19%) and α_2 and λ (17%), either by the direct effect or interactions with other parameters.

For KGE_rc, the n_2 and n_1 parameters show a relatively significant direct effect (18% and 11%). Other parameters have first-order indices less than 10%, indicating that their direct effect on the variance of KGE_rc is relatively small. The sum of all first-order indices is less than 1, and about 46% of the variance is caused by the direct effects, suggesting that the interactions between parameters are very important. About 35% of the variance of KGE_rc is caused by n_2, followed by n_3 (29%) and n_1 (25%), either by the direct effect or interactions with other parameters.

For KGE_avg, the n_2 and n_1 parameters show a relatively significant direct effect (22% and 12%). Other parameters have first-order indices less than 10%, indicating that their direct effect on the variance of KGE_avg is relatively small. The sum of all first-order indices is less than 1, and about 48% of the variance is caused by the direct effects, suggesting that the interactions between parameters are very

important. About 39% of the variance of KGE_avg is caused by n_2, followed by n_1 (27%) and n_3 (22%), either by the direct effect or interactions with other parameters.

The total sensitivity index of all parameters is always greater than zero, which means that none of the parameters can be fixed because they affect the output variance either directly or by their interactions. Overall, as seen from the KGE_avg sensitivity analysis results, the order of sensitive parameters is as follows: shape parameters *n*, shape parameters α, saturated water contents θ_s, saturated hydraulic conductivities K_s, and dispervities λ.

Overall, the qualitative ranking based on the Morris method is consistent with quantitative indices obtained by the Sobol' method, which confirms that the sensitivity analysis results are reliable.

S1.2 Monte Carlo filtering

A Monte Carlo filtering produced a filtered sample of 87 good solutions with KGE_bf, KGE_wc, KGE_wi, KGE_rc, KGE_avg=0 as the threshold value. Scatter plots for the parameters of different soil layers and the convergent solutions for the average model performance (KGE_avg) are displayed in Fig. S2, S3, and S4, respectively. For the first layer (Fig. S2), KGE_avg decreases as θ_{s1}, α_1, n_1, and λ increase, and increases as K_{s1} increases, although with very different correlation coefficients. More plausible solutions lie in the left part (1.1~1.4) of the scatter plot for the n_1 parameter. For the second layer (Fig. S3), KGE_avg decreases as n_2, K_{s2}, and λ increase, and increases as θ_{s2} and α_2 increase, again, with very different correlation coefficients. More plausible solutions lie in the left part (1.1~1.4) of the scatter plot for the n_2 parameter. For the third layer (Fig. S4), KGE_avg decreases as θ_{s3}, α_3, and λ increase, and increases as n_3 and K_{s3} increase.

The univariate and bivariate plots for different soil layers (Figs. S5~S7) reveal significant information about reasonable ranges of parameters. Leptokurtic distributions in the univariate KDE plots generally indicate low uncertainty and are often observed for highly sensitive parameters. It means that observations are informative for these parameters, and therefore, they can be estimated with good confidence. We can further compare the bivariate KDE plots and get the parameter ranges of other related variables using this information.

For the first layer (Fig. S5), the maximum correlation coefficients (in absolute values) are 0.40 for the α_1 and n_1 parameters and 0.30 for the α_1 and θ_{s1} parameters. The correlation between other parameters is relatively small. The univariate KDE for the parameters n_1 and α_1 (the most sensitive parameters for the first layer) exhibit a leptokurtic distribution, and their good solutions clearly concentrate in 1.1~1.4 and 0.001~0.2, respectively. The bivariate KDE for n_1-α_1 again highlights a denser region for α_1 in 0.001~0.2. The bivariate KDE for α_1-θ_{s1} and n_1-θ_{s1} highlight a denser region for θ_{s1} in 0.3~0.5.

For the second layer (Fig. S6), the maximum correlation coefficient (in absolute values) is 0.34 between the α_2 and n_2 parameters. The correlation between other parameters is relatively small. The univariate KDE for the parameters n_2 and α_2 (the most sensitive parameters for the first layer) exhibit a leptokurtic distribution, and their good solutions clearly concentrate in 1.1~1.4 and 0.1~0.3, respectively. The bivariate KDE for n_2-α_2 again highlights a denser region for α_2 in 0.1~0.3. The bivariate KDE for n_2-λ highlights a denser region for λ in 5~20. The bivariate KDE for α_2-K_{s2} highlights a denser region for K_{s2} in 10~9000. The bivariate KDE for α_2-θ_{s2} highlight a denser region for θ_{s1} in 0.4~0.6.

For the third layer (Fig. S7), the maximum correlation coefficients (in absolute values) are 0.60 for the α_3 and n_3 parameters, and 0.41 for the α_3 and θ_{s3} parameters. The correlation between other parameters is relatively small. No other significant information about the possible ranges of parameters can be found.

The results of the multivariate plot analysis were used to reduce the ranges of parameters for the following optimization process (Table S2). The reduction was only applied to parameters that showed well identifiable good solution regions.

Results S2: Global sensitivity analysis and Monte-Carlo filtering for the Braud et al. (2009a) dataset

S2.1 Global sensitivity analysis

a. Morris method

Table S4 provides the initial ranges of all evaluated parameters. Fig. S11 reports the order of sensitive parameters for the soil water content (KGE_wc), water isotopic composition (KGE_wi), and the average (KGE_avg). It can be seen from the μ_j^* values that the n and θ_s parameters show a significant direct effect on the outputs, followed by the K_s and α parameters, while λ parameter has the smallest direct effect. All parameters with high direct effects (large μ_j^*) often have high indirect effects (large σ_j). The $\mu_j^* \sim \sigma_j$ values plot around or above the 1:1 line, suggesting that the indirect effects or interactions between parameters are close to or more significant than the direct effects.

b. Sobol' method

Table S5 reports sensitivity indices for the isotopic composition of soil water. For KGE_wc and KGE_wi, n, and θ_s, parameters show a relatively significant direct effect (38%, and 31%, respectively). Other parameters have first-order indices less than 10%, indicating that their direct effect on the variance of KGE_bf is relatively small. The sum of all first-order indices is less than 1, and about 69% of the variance is caused by the direct effects, suggesting that the interactions between parameters are relatively small. To sum up, about 69% of the variance of KGE_wc is caused by n, followed by θ_s (60%) and λ (14%), either by the direct effect or interactions with other parameters. For KGE_avg, only n parameter show a relatively significant direct effect (63%). Other parameters have first-order indices less than 10%, indicating that their direct effect on the variance of KGE_avg is relatively small. The sum of all first-order indices is less than 1, and about 67% of the variance is caused by the direct effects, suggesting that the interactions between parameters are relatively small. To

sum up, about 98% of the variance of KGE_wc is caused by n, followed by θ_s (35%), either by the direct effect or interactions with other parameters.

The total sensitivity index of all parameters is always greater than zero, which means that no parameters can be fixed because they affect the output variance directly or by their interactions. Overall, as observed from the KGE_avg sensitivity analysis results, the most sensitive parameters are shape parameters n and saturated water contents θ_s.

Overall, the qualitative ranking based on the Morris method is in general consistent with quantitative indices obtained by the Sobol' method, which provides additional confirmation that the sensitivity analysis results are reliable.

S2.2 Monte Carlo filtering

The univariate and bivariate plots do not reveal significant information about reasonable ranges of parameters and thus are not shown here. The reduced ranges of parameters for the following optimization process are shown in Table S4.

References

Nossent, J., Elsen, P., Bauwens, W., 2011. Sobol' sensitivity analysis of a complex environmental model. Environ. Modell. Softw. 26 (12), 1515–1525. doi:10.1016/j.envsoft.2011.08.010.

Sobol, I.M., 2001. Global sensitivity indices for nonlinear mathematical models and their Monte Carlo estimates. Math. Comput. Simul. 55 (1–3), 271–280. doi:10.1016/s0378-4754(00)00270-6.